

Electronic Supplementary Information

Recognition and optical sensing of amines by a quartz-bound 7-chloro-4-quinolylazopillar[5]arene monolayer

Ilenia Pisagatti,^a Giuseppe Gattuso,^a Anna Notti,^a Melchiorre F. Parisi,^{*a}
Giovanna Brancatelli,^{‡b} Silvano Geremia,^b Francesco Greco,^{c,d} Salvatrice Millesi,^{c,d}
Andrea Pappalardo^{c,d} Luca Spitaleri,^{c,d} and Antonino Gulino^{*c,d}

^aDipartimento di Scienze Chimiche, Biologiche, Farmaceutiche ed Ambientali, Università di Messina, Viale F. Stagno d'Alcontres 31, 98166 Messina, Italy. E-mail: mparisi@unime.it

^bCentro di Eccellenza in Biocristallografia, Dipartimento di Scienze Chimiche e Farmaceutiche, Università di Trieste, via L. Giorgieri 1, 34127 Trieste, Italy.

^cDipartimento di Scienze Chimiche, Università di Catania, Viale Andrea Doria 6, 95125 Catania, Italy. E-mail: agulino@unict.it

^dI.N.S.T.M. UdR of Catania, Viale Andrea Doria 6, 95125 Catania, Italy.

[‡] Current address: Crystallics B.V., Meibergdreef 31, 1105 AZ, Amsterdam, The Netherlands.

Contents	page
X-ray Studies	S2
Table S1 Crystal data and structure refinement for QAP5	S3
Fig. S1 The crystal structure of QAP5	S4
Fig. S2 The molecular packing of QAP5	S4
Fig. S3 ¹ H NMR spectrum of QAP5	S5
Fig. S4 HSQC NMR spectrum of QAP5	S5
Fig. S5 AFM micrograph of QAP5 _ML	S6
Fig. S6 UV-vis spectra of QAP5 and QAP5 _ML in different solvents	S6
Fig. S7 UV-vis spectra of 7-chloro-4-quinolylazophenol upon addition of <i>n</i> -butylamine	S7
Fig. S8 UV-vis titration experiment of QAP5 with <i>n</i> -butylamine	S7
Fig. S9 UV-vis titration experiment of QAP5 with 1,8-diaminooctane	S7
Fig. S10 UV-vis titration experiment of QAP5 with dansylcadaverine	S7
Fig. S11 ¹ H NMR titration experiment of QAP5 with 1,8-diaminooctane	S8
Fig. S12 Non-linear curve-fitting of the ¹ H NMR titration data (QAP5 / 1,8-diaminooctane)	S8
Fig. S13 Emission titration spectra of dansylcadaverine upon addition of QAP5	S9
Fig. S14 Non-linear curve-fitting of the emission intensity changes QAP5 with dansylcadaverine	S9

X-ray Studies

Crystal Structure Determination of pillar[5]arene QAP5: data collections were carried out at the Macromolecular Crystallography XRD1 beamline of the Elettra synchrotron (Trieste, Italy), by employing the rotating-crystal method and the cryo-cooling technique. Routinely a crystal dipped in Paratone®, as cryo-protectant, was mounted on a loop and immediately flash-frozen under a liquid nitrogen stream at a 100 K. The diffraction data of QAP5 were indexed and integrated using the XDS package.¹ Scaling was carried out with XSCALE.²

The crystal analyzed was rather small and, as a result, it was necessary to use a synchrotron radiation coupled with cryo-cooling techniques to collect a dataset of sufficient quality to solve and refine the structure. The structure was solved by direct methods using SIR2011.³ Non-hydrogen atoms at full occupancy, or with population equal to, or higher than, 0.6 were anisotropically (hydrogen atoms added at the calculated positions, excluded the solvent molecules) refined by full-matrix least-squares methods on F² using SHELXL-13.⁴ Restraints on the geometrical and thermal parameters of the disordered solvent molecules (DFIX, SIMU) were introduced during the last refinement cycles.

The structure of **QAP5** showed severe disorder, especially in the solvent component: tetrachloroethane molecules were refined at 0.7 of partial occupancy and the -CHCl₂ groups were seen to adopt two different orientations, both refined at equal occupancy. Nine methanol molecules were located: one at full occupancy (the one bridging two adjacent pillar[5]arene molecules), one refined at 0.6, one disordered over three positions refined at 0.5, 0.25, 0.25, respectively, one was found disordered over two positions refined at 0.35 and 0.4, respectively and the last one was refined at 0.4 of partial occupancy. Also a water molecule was refined at half occupancy. Among solvent molecules, hydrogen atoms were added only on the methanol at full occupancy and on the tetrachloroethane molecule. Crystallographic data and refinement details are reported in Table S1.

1 W. Kabsch, *Acta Crystallogr.*, 2010, **D66**, 125–132.

2 W. Kabsch, *Acta Crystallogr.*, 2010, **D66**, 133–144.

3 M. C. Burla, R. Caliandro, M. Camalli, B. Carrozzini, G. L. Casciarano, L. De Caro, C. Giacovazzo, G. Polidori, D. Siliqi and R. Spagna, *J. Appl. Crystallogr.*, 2007, **40**, 609–613.

4 G. M. Sheldrick, *Acta Crystallogr.*, 2008, **A64**, 112–122.

Table S1 Crystal data and structure refinement for **QAP5**

QAP5	
Empirical formula	C ₅₂ H ₅₀ N ₃ O ₉ Cl, 4.25 (CH ₃ OH), 0.7 (C ₂ H ₂ Cl ₄), 0.5 H ₂ O
Formula weight	1159.1 ^a
Temperature (K)	100(2)
Wavelength (Å)	0.8000
Crystal system	Monoclinic
Space group	<i>P</i> 2 ₁ /n
Unit cell dimensions (Å, °)	<i>a</i> = 12.576(2), α = 90 <i>b</i> = 33.286(1), β = 95.981(3) <i>c</i> = 14.585(2), γ = 90
Volume (Å ³)	6072.1(13)
Z	4
ρ_{calcd} (g/cm ³)	1.268 ^a
μ (mm ⁻¹)	0.339
F(000)	2443.6 ^a
Reflections collected	39700
Independent reflections	11904 [R(int) = 0.0878]
Data / restraints / parameters	11904 / 20 / 784
GooF	1.043
Final <i>R</i> indices [<i>I</i> > 2 σ (<i>I</i>)]	<i>R</i> ₁ = 0.1059, <i>wR</i> ₂ = 0.2726
<i>R</i> indices (all data)	<i>R</i> ₁ = 0.1096, <i>wR</i> ₂ = 0.2763
CCDC code	1536000

^a The FW, density and F(000) were corrected by taking also into account the hydrogen atoms present in the water and methanol molecules not included in the crystallographic model.

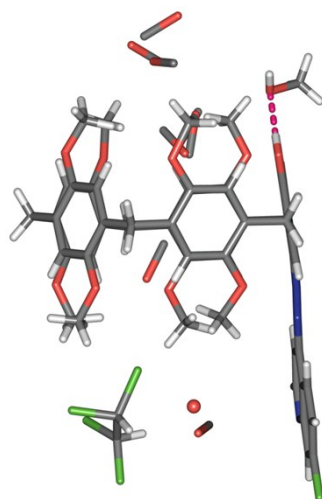
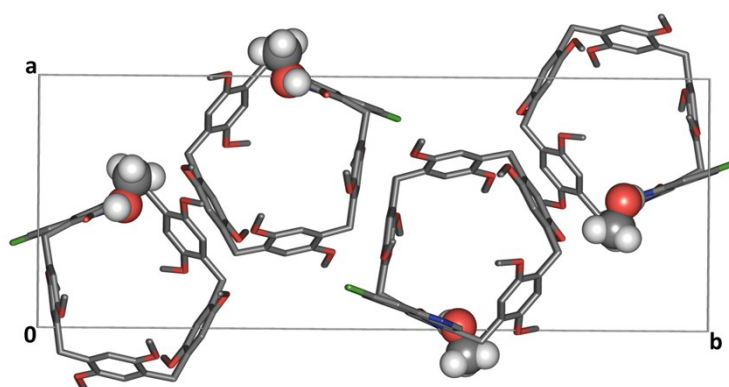


Fig. S1 The asymmetric unit of the crystal structure of quinolyazo-pillar[5]arene **QAP5** showing the presence of several disordered methanol molecules within the cavity and its vicinity. A disordered tetrachloroethane molecule is also seen next to the quinolyazo moiety.

a)



b)

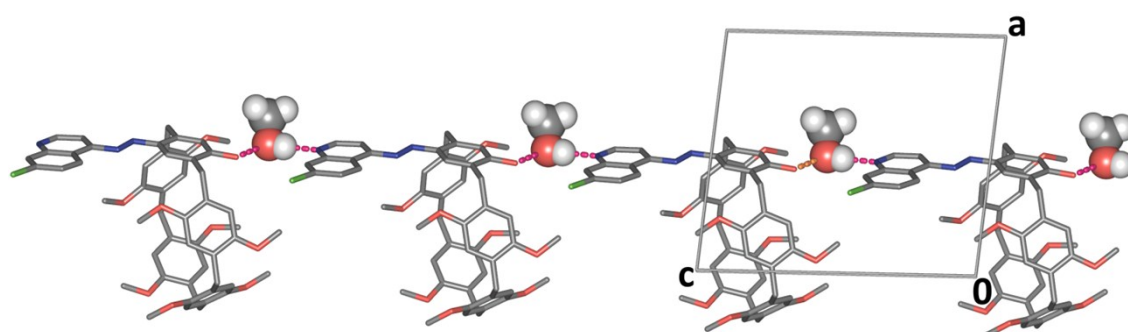


Fig. S2 One-dimensional channels seen in the molecular packing of **QAP5**: a) view of the pentagonal-shaped channels, orthogonal to the *ab* plane and b) view along the *c* axis of the pillar[5]arene molecules; channel propagation is provided by bridging methanol molecules concomitantly acting as hydrogen-bond acceptors ($\text{OH}\cdots\text{O}_{\text{Me}}$ 2.647(3) Å) and hydrogen-bond donors ($\text{OH}_{\text{Me}}\cdots\text{N}$ 2.717(4) Å). The bridging methanol molecules are conveniently depicted with Van der Waals spheres.

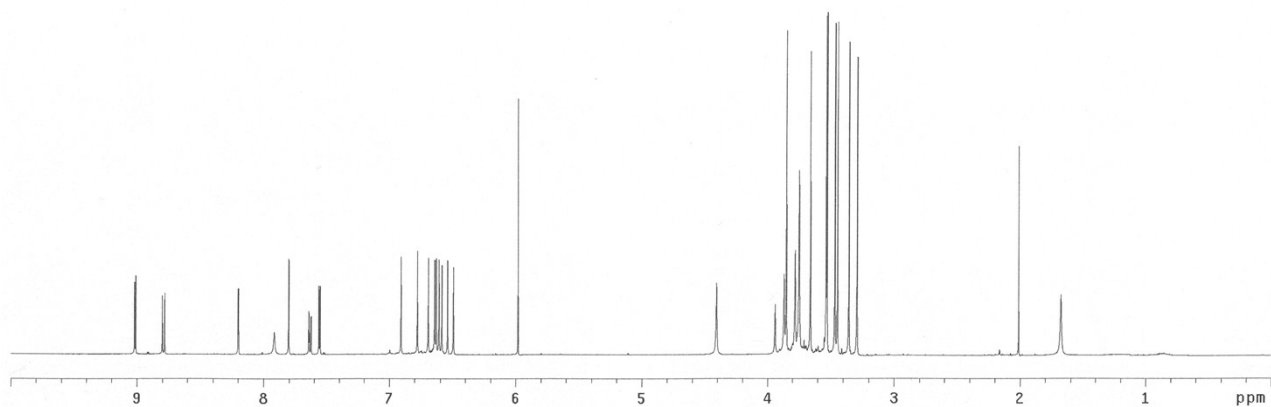


Fig. S3 ^1H NMR spectrum (500 MHz, TCE-d_2 , 298 K) of 7-chloro-4-quinolyazo-octamethoxypillar[5]arene (QAP5).

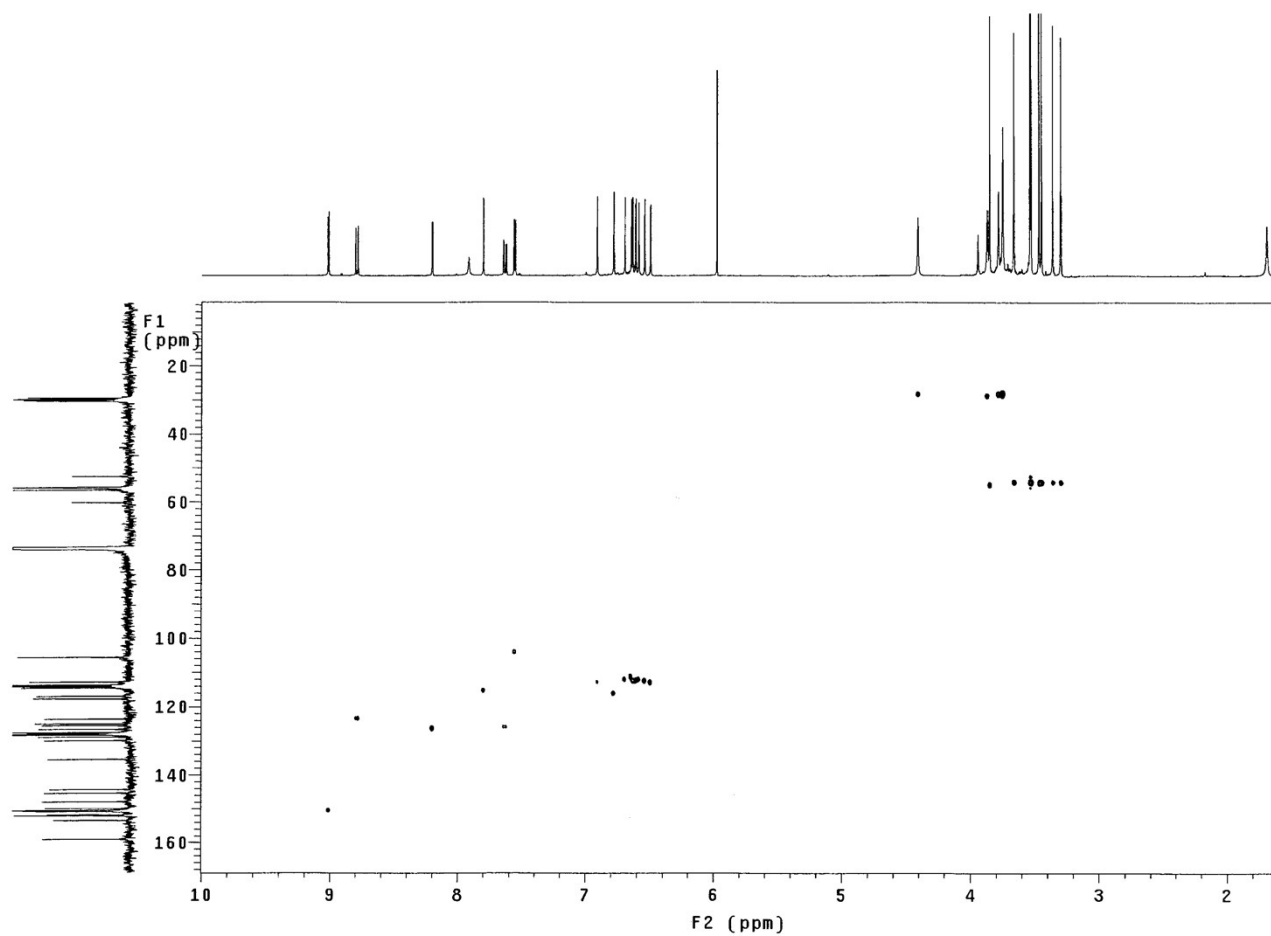


Fig. S4 HSQC NMR spectrum (TCE-d_2 , 298 K) of 7-chloro-4-quinolyazo-octamethoxy-pillar[5]arene (QAP5).

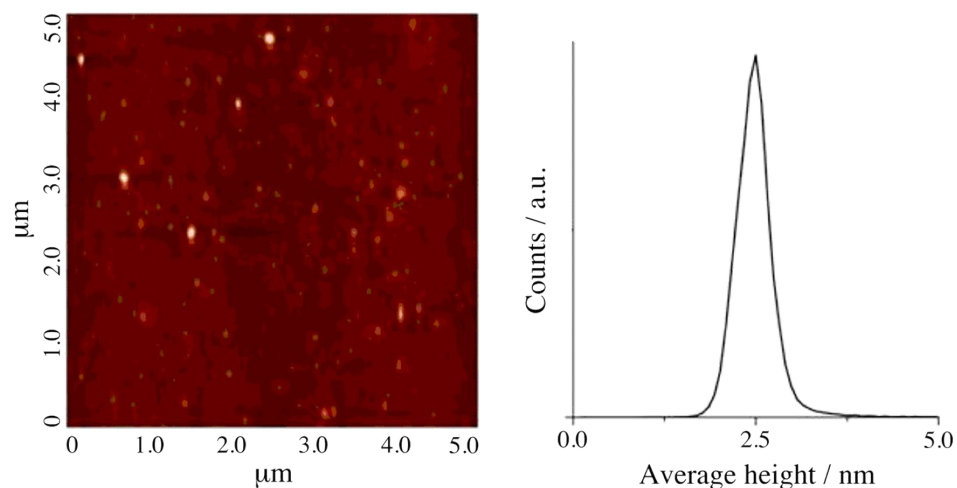


Fig. S5 AFM micrograph of a representative **QAP5_ML** (left) and related cross-section profile (right).

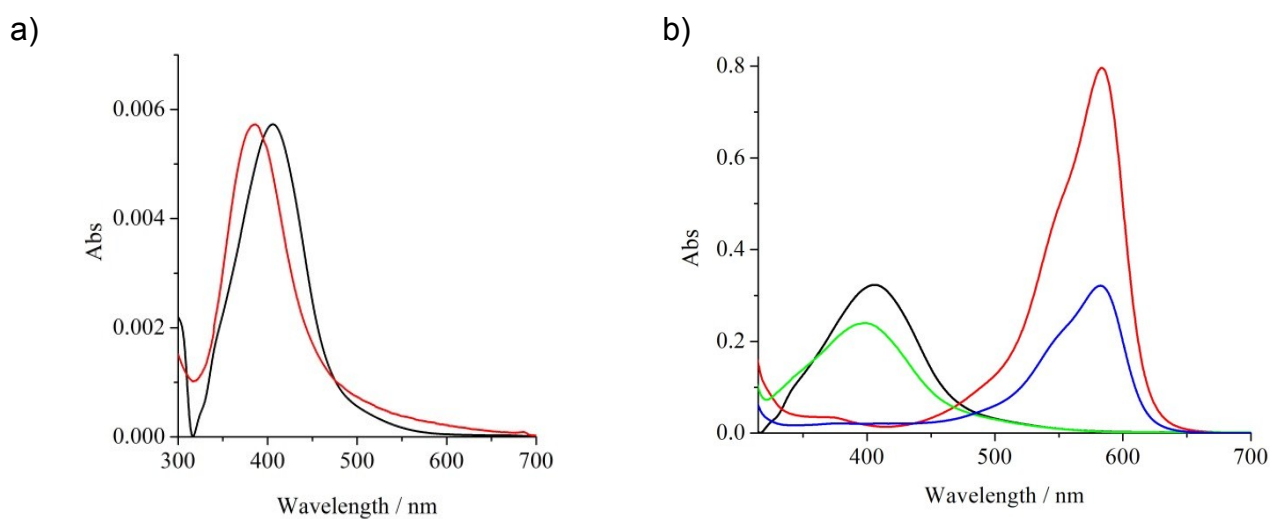


Fig. S6 UV-vis spectra of: a) a 1.8×10^{-7} M **QAP5** toluene solution (black trace) and a **QAP5_ML** (red trace); b) 1.0×10^{-5} M **QAP5** solutions in DMSO, TCE and toluene (red, green and black traces, respectively). The additional blue trace refers to a 2.1×10^{-5} M DMSO solution of **QAP5** as the sodium salt.⁵

⁵ The sodium salt of **QAP5** was obtained by treating **QAP5** with a NaOH (1 equiv) H₂O/DMSO (1:1) solution, upon solvent removal under reduced pressure.

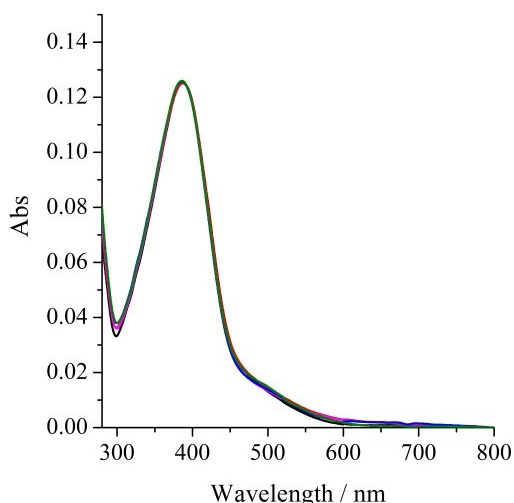


Fig. S7 UV-vis spectra of a 1.07×10^{-5} M TCE solution of 4-(7-chloro-4-quinolylazo)-2,5-dimethylphenol (**QA**) upon subsequent additions of a 1.43×10^{-3} M TCE solution of *n*-butylamine (up to 100 equiv).

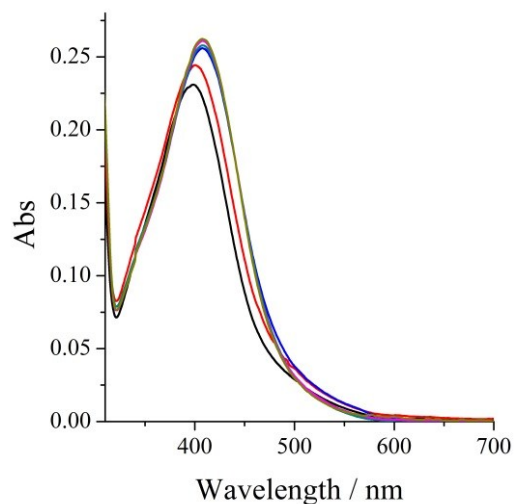


Fig. S8 UV-vis titration experiment of a TCE solution of **QAP5** (1.0×10^{-5} M) with a 1.33×10^{-3} M TCE *n*-butylamine solution: $[\text{QAP5}] / [n\text{-butylamine}] = 1:0, 1:1, 1:5, 1:10, 1:20$ and $1:50$; black, red, blue, cyan, magenta and yellow traces, respectively. All spectra have been corrected for the volume variation.

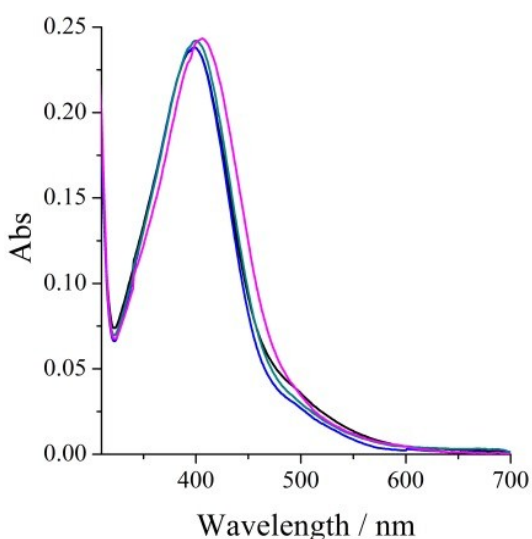


Fig. S9 UV-vis titration experiment of a TCE solution of **QAP5** (1.0×10^{-5} M) with a 1.33×10^{-3} M TCE 1,8-diaminooctane solution: $[\text{QAP5}]/[1,8\text{-diaminooctane}] = 1:0, 1:5, 1:10,$ and $1:100$; black, blue, cyan, and magenta traces, respectively. All spectra have been corrected for the volume variation.

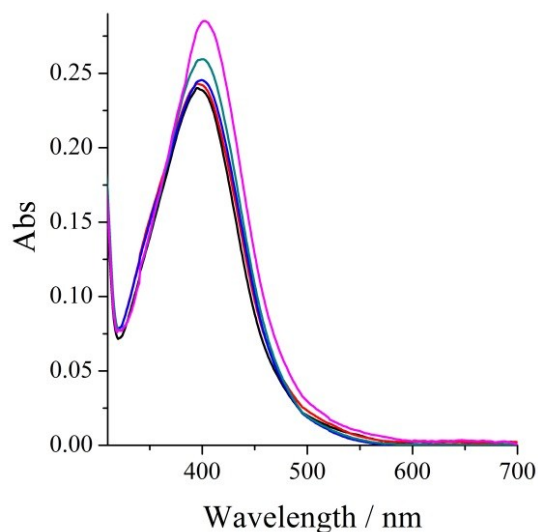


Fig. S10 UV-vis titration experiment of a TCE solution of **QAP5** (1.0×10^{-5} M) with a 1.33×10^{-3} M TCE dansylcadaverine solution: $[\text{QAP5}]/[\text{dansylcadaverine}] = 1:0, 1:10, 1:50$ and $1:100$; black, red, blue, green, and magenta traces, respectively. All spectra have been corrected for the volume variation.

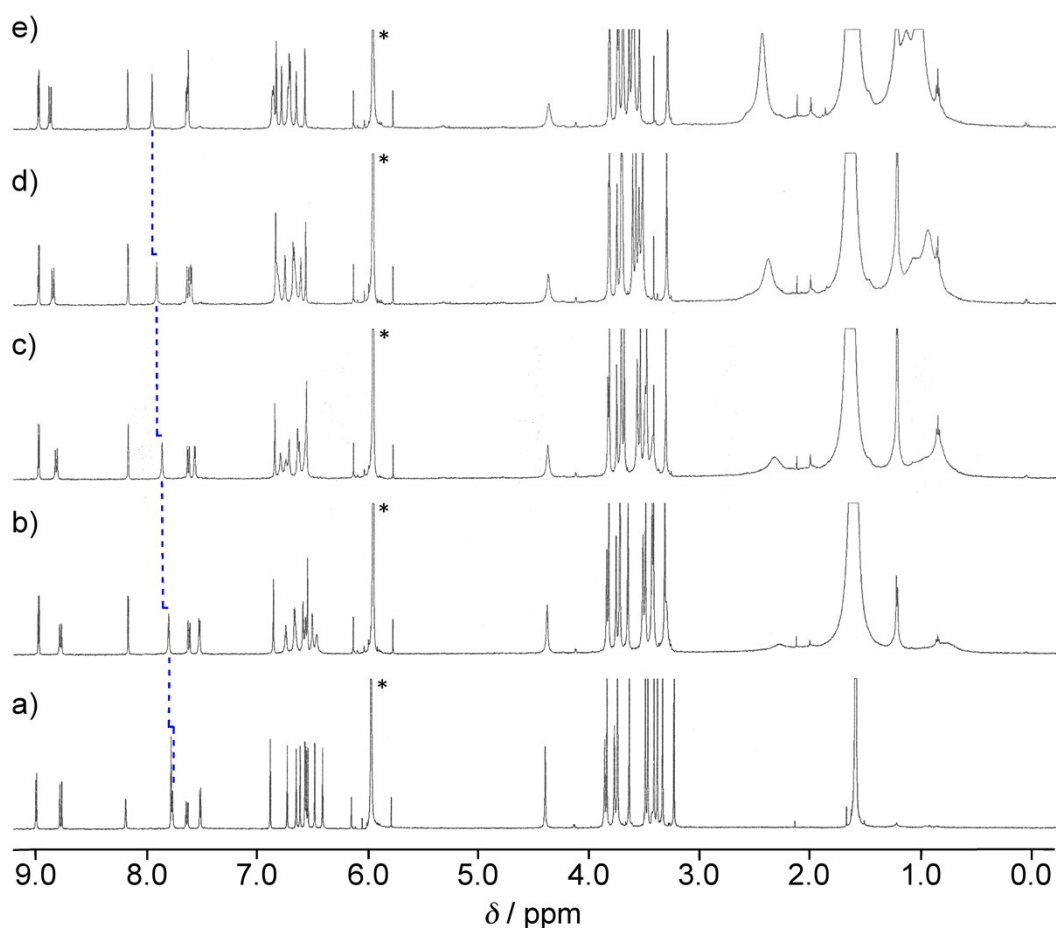


Fig. S11 ^1H NMR spectra (500 MHz, $\text{TCE-}d_2$, 298 K) of a) **[QAP5]** = 1.0 mM; b) **[QAP5]** = 1.0 and **[1,8-diaminooctane]** = 0.4 mM; c) **[QAP5]** = 1.0 and **[1,8-diaminooctane]** = 1.3 mM; d) **[QAP5]** = 1.0 and **[1,8-diaminooctane]** = 2.8 mM and e) **[QAP5]** = 1.0 and **[1,8-diaminooctane]** = 4.7 mM. Asterisks designate the residual solvent peak.

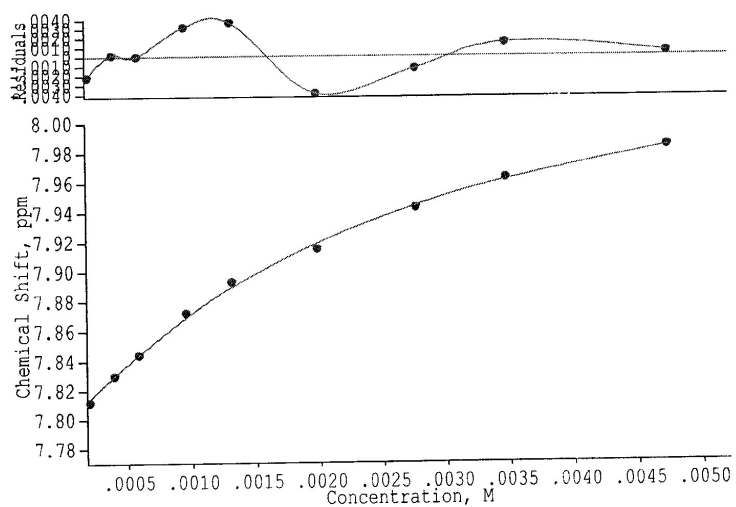


Fig. S12 Non-linear curve-fitting of the ^1H NMR (500 MHz, 298 K) chemical shift changes of a 1.0 mM $\text{TCE-}d_2$ solution of **QAP5** upon addition of increasing amounts of 1,8-diaminooctane.

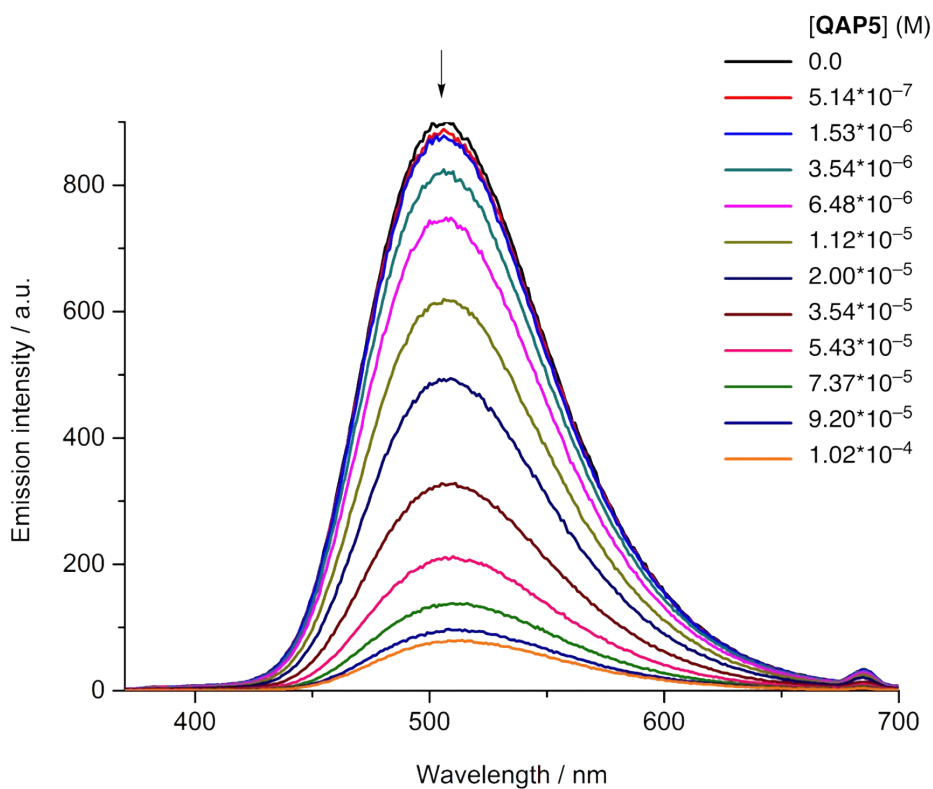


Fig. S13 Emission titration spectra ($\lambda_{exc} = 340$ nm) of a TCE solution of [dansylcadaverine] = 9.9×10^{-6} M upon addition of increasing amounts of a QAP5 TCE solution at 25 °C.

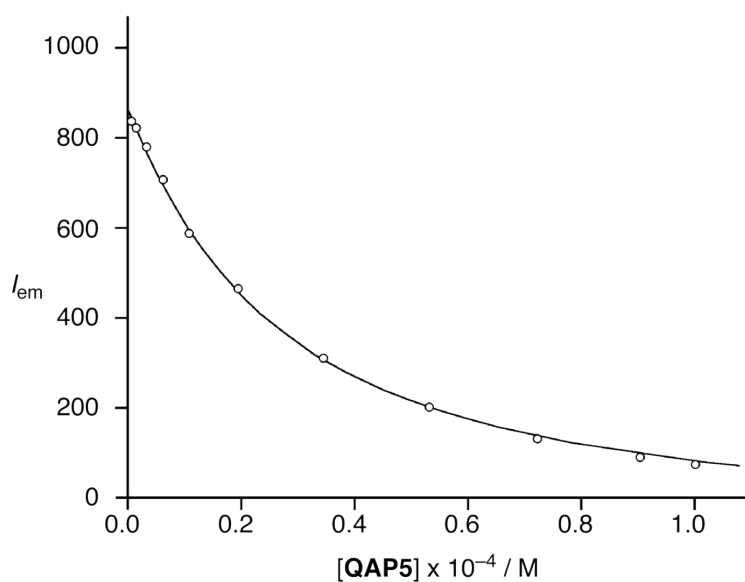


Fig. S14 Non-linear curve-fitting of the emission intensity changes ($\lambda = 510$ nm) of a TCE solution of [dansylcadaverine] = 9.9×10^{-6} M upon addition of increasing amounts of a QAP5 TCE solution.